

Isomeric states in proton-unbound $^{187,189}\text{Bi}$ isotopes

A. Hürstel¹, M. Rejmund¹, E. Bouchez¹, P.T. Greenlees², K. Hauschild¹, S. Juutinen², H. Kettunen², W. Korten^{1,a}, Y. Le Coz¹, P. Nieminen², Ch. Theisen¹, A.N. Andreyev³, F. Becker^{1,b}, T. Enqvist², P.M. Jones², R. Julin², H. Kankaanpää², A. Keenan², P. Kuusiniemi², M. Leino², A.-P. Leppänen², M. Muikku^{2,c}, J. Pakarinen², P. Rahkila², and J. Uusitalo²

¹ DAPNIA/SPhN CEA-Saclay 91191 Gif-sur-Yvette Cedex, France

² JYFL, University of Jyväskylä, Finland

³ Department of Physics, University of Liverpool, UK

Received: 2 May 2002 /

Published online: 19 November 2002 – © Società Italiana di Fisica / Springer-Verlag 2002

Communicated by D. Schwalm

Abstract. Prompt and delayed gamma-ray spectroscopy of very neutron-deficient bismuth isotopes $^{187,189}\text{Bi}$ has been performed using the Recoil Decay Tagging (RTD) method. The isomeric $i_{13/2}$ states have been identified and their lifetimes have been measured. The systematics of these long-lived $M2$ isomers has been extended to the proton-unbound isotopes. The general behaviour of single-proton states is discussed within the systematics and interpreted within the shell-model framework.

PACS. 23.20.Lv Gamma transitions and level energies – 27.70.+q $150 \leq A \leq 189$ – 21.10.Tg Lifetimes

1 Introduction

Shape coexistence of a spherical ground state and low-lying deformed states has been established in neutron-deficient lead isotopes. Around the neutron mid-shell, the unique feature of a triple shape coexistence has been observed in $^{186,188}\text{Pb}$ [1–3] with prolate and oblate excited 0^+ states being close in excitation energy. The deformed states have been interpreted to be due to the occupation of proton intruder orbitals which are well known to occur at rather low excitation energy in the mass-190 region [4].

The identification of the proton orbitals involved is necessary to better understand the microscopic origin of shape coexistence in this mass region. Such information cannot be deduced from the study of the 0^+ states in even-even lead isotopes where pairs of protons are coupled. Therefore, the orbitals which are responsible for driving the nucleus towards deformation are better investigated through a study of the valence proton excitations in the neighbouring odd- A isotopes. This can be achieved by studying the isotopes $^{187,189}\text{Bi}$, which correspond to a single proton added to the respective $^{186,188}\text{Pb}$ cores.

In neutron-deficient odd- A bismuth isotopes, down to ^{187}Bi , the spin and parity of the ground state have been

established to be $9/2^-$. Two particular low-lying isomers are observed in these isotopes. An excitation of a proton across the $Z = 82$ shell gap leads to a low-lying excited $1/2^+$ state. A second isomer, due to the excitation of the valence proton, has a spin-parity $13/2^+$ [5]. Recent mass measurements [6] have shown that ^{189}Bi is the first isotope of the odd- A bismuth chain where the proton separation energy changes its sign, *i.e.* the last proton is only quasi-bound by the Coulomb potential while ^{185}Bi has been found to be a proton emitter [7,8].

In this work, the systematics of isomeric states in odd- A bismuth isotopes has been extended to ^{187}Bi . For $187 \leq A \leq 209$, the behaviour of the $9/2^-$ and $13/2^+$ states has been studied in the potential of the corresponding lead core. The properties of the $M2$ transitions occurring in $^{187,189}\text{Bi}$ and connecting the $13/2^+$ state to the $9/2^-$ ground state are also discussed within the systematics.

2 Experiments and results

The experiments were performed using the K130 cyclotron facility at the University of Jyväskylä (Finland). The nuclei of interest were populated in fusion-evaporation reactions of $^{82,83}\text{Kr}$ beams with $^{107,109}\text{Ag}$ targets. The yield of these nuclei far from stability, into the region where the last proton is no longer bound, is strongly reduced by fission competition and charged-particle emission. This makes a

^a e-mail: wkorten@cea.fr

^b Present address: GANIL, Caen, France.

^c Present address: Radiation and Nuclear Safety Authority, P.O. Box 14, FIN-00881 Helsinki.

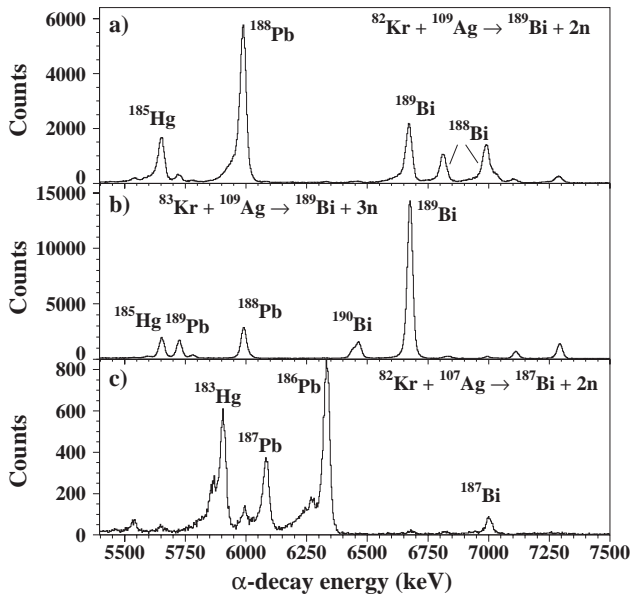


Fig. 1. α -particles energy spectra measured in the a) first, b) second and c) third experiment. See text for further explanations.

separation and identification of the reaction products necessary. For this purpose we have used the very selective technique of Recoil Decay Tagging (RDT) which is based on the time and position correlation of a fusion evaporation residue and its characteristic α -decay [9].

The fusion-evaporation residues, separated in flight from scattered beam and fission products by the gas-filled separator RITU [10], were implanted in a position-sensitive silicon detector (PSSD) located at the focal plane of the separator. The 35×80 mm (vertical \times horizontal) silicon detector was divided horizontally into 16 resistive strips. Vertically, *i.e.* along the strips, an average position resolution of ~ 500 μm has been achieved. The energy resolution for 6 MeV α -particles was ~ 30 keV. The energy, time and position of the implanted residues and their subsequent α -decay were recorded. Data were written on tape if a signal in the PSSD was registered.

Around the target, prompt γ -rays were detected by the Jurosphere II array. The beam intensity was therefore limited to ~ 10 pA by the counting rate in the Ge detectors. Results on prompt γ -ray spectroscopy will be discussed in a forthcoming paper [11].

The time of flight of the fusion-evaporation residues through the separator was ~ 400 ns making it possible to study isomers with a half-life greater than a few hundred ns by delayed spectroscopy at the focal plane of the separator. The delayed γ -ray transitions were detected by two different setups placed behind the PSSD detector. In the first and third experiment a Ge detector with an efficiency of $\sim 0.6\%$ at 1.3 MeV was used. A BGO wall composed of 14 crystals closely packed giving a high efficiency of about 15% and an energy resolution of $\sim 20\%$ was used for the second experiment. In both cases the energy and time of the delayed γ -rays were recorded within a time window of 32 μs after a PSSD signal.

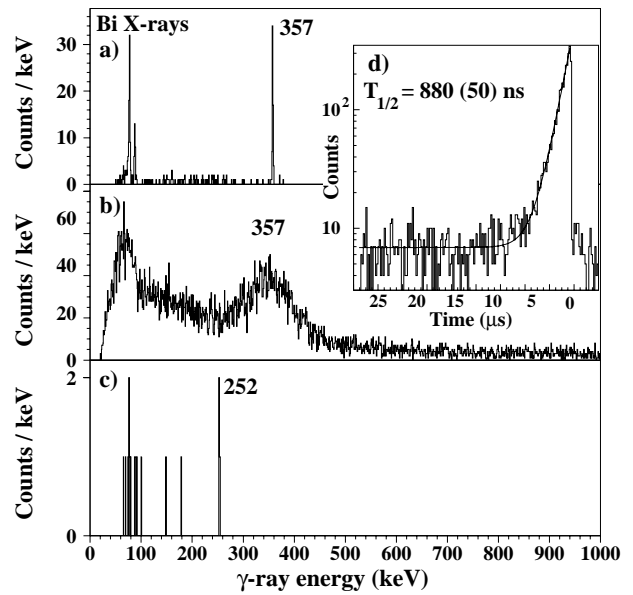


Fig. 2. Spectra of delayed γ -rays measured at the focal plane of the RITU separator. Recoil decay tagging has been applied to the ground-state α -decays of a) and b) ^{189}Bi and c) ^{187}Bi . d) Time distribution of the 357 keV transition.

In the first experiment the isotope ^{189}Bi was produced via a 2n evaporation channel in the fusion reaction of a ^{82}Kr beam at 337 MeV in the middle of the target (MOT) and a $960 \mu\text{g}/\text{cm}^2$ thick ^{109}Ag target. We collected about 25000 events with an α -particle energy of 6674(5) keV corresponding to the known ground-state α -decay of ^{189}Bi [12] (see fig. 1a). The half-life was determined to be 667(13) ms, in agreement with previous results [12,13]. The dominant α -decay line observed in this experiment at 5983 keV is the ground-state α -decay of ^{188}Pb , even though the alpha branching ratio from this nucleus is only about 10% [14]. This clearly shows the predominant production of ^{188}Pb in this reaction via the p2n channel. Therefore we repeated the experiment using a ^{83}Kr beam at 340 MeV (MOT) on a $1.06 \text{ mg}/\text{cm}^2$ thick ^{109}Ag target. In this way the production cross-section for ^{189}Bi in the 3n evaporation channel could be increased by a factor of ~ 6 . About 140000 events with a 6674 keV α -particle were collected (see fig. 1b). In contrast to the first experiment, the peak identifying the ground-state α -decay of ^{189}Bi dominates.

The spectra of delayed γ -rays coincident with recoils that were correlated with the 6674 keV α -decay in a time window of 2 s, are presented in the upper two panels of fig. 2. In the spectrum of fig. 2a (obtained in the first experiment with a single Ge detector) only a single γ -line with an energy of 357 keV is observed, which has been previously observed and assigned to ^{189}Bi [15]. In addition, this spectrum contains only Bi X-rays, confirming the correct identification of the isotope. In the second experiment, a high-efficiency BGO wall replaced the Ge detector at the focal plane in order to increase the statistical accuracy of the data. The 357 keV γ -ray is again clearly distinguishable (fig. 2b). From the corresponding

time distribution, containing ~ 5000 counts, a half-life of 880(50) ns was determined (see fig. 2d).

In the third experiment, the nucleus ^{187}Bi was studied using a ^{82}Kr beam at 339 MeV (MOT) and a 1.13 mg/cm^2 thick ^{107}Ag target. The energy spectrum of the α -particles is shown in fig. 1c. The known ground-state decay of ^{187}Bi at 7000(5) keV [16] is clearly visible. From the time distribution of the α -particles containing about 1000 events a half-life of 45(11) ms was deduced, which is somewhat longer than the value of 32(3) ms published in ref. [16]. The dominant line at 6332 keV is from ^{186}Pb , produced in the p2n channel, a situation similar to the first experiment. The production cross-section of ^{187}Bi is estimated to be less than 100 nbarn, which is a factor of 40 less than obtained for ^{189}Bi under similar experimental conditions. The spectrum of delayed γ -rays, obtained with the condition of an α -recoil correlation within a time window of 150 ms, is shown in fig. 2c. Four events containing a new 252 keV γ -transition were observed. This is the first observation of an excited (isomeric) state that decays by γ -rays in ^{187}Bi . A half-life of $3.2_{-2.0}^{+7.6} \mu\text{s}$ has been deduced using the procedure described in ref. [17] to deduce lifetimes from a small number of events.

We would like to emphasise that in both isotopes the γ -decays are firmly established to feed the corresponding ground states since a clear identification using the RDT method has been made. It should also be noted that no other γ -rays have been seen at the focal plane of the separator in correlation with $^{187,189}\text{Bi}$ recoils.

3 Discussion

The proton configurations relevant in odd- A bismuth isotopes are shown schematically in the upper part of fig. 3. The $9/2^-$ ground-state configuration is interpreted to be mainly the valence $1h_{9/2}$ proton coupled to the spherical 0^+ state of the underlying lead core. The excited $1/2^+$ state is due to a proton excitation across the $Z = 82$ shell gap, *i.e.* from $s_{1/2}$ to the $h_{9/2}$ orbital [18] leading to a $2p-1h$ configuration. Isomeric transitions feeding the $9/2^-$ ground state are observed in all light bismuth isotopes starting from ^{195}Bi [19]. They are generally found to be magnetic quadrupole ($M2$) transitions from a $13/2^+$ isomer, which has been interpreted as a proton excitation into the $i_{13/2}$ valence orbital [20].

With our new results, the systematics of $|\pi i_{13/2}; 13/2^+\rangle$ isomers in odd- A bismuth isotopes has been extended down to ^{187}Bi . The isomeric $13/2^+$ state in ^{189}Bi at 357 keV has been previously observed, but we could determine for the first time a half-life of 880(50) ns. This is in agreement with the lower limit given in ref. [15]. In ^{187}Bi we have observed a new isomeric state at 252 keV with a half-life of $3.2_{-2.0}^{+7.6} \mu\text{s}$. The assignment as $13/2^+$ states is also supported by the measured half-lives, which are typical for low-energy $M2$ transitions in this mass region. In view of the small transition energies only a small admixture of an $E3$ component is expected in the transitions. A rather pure

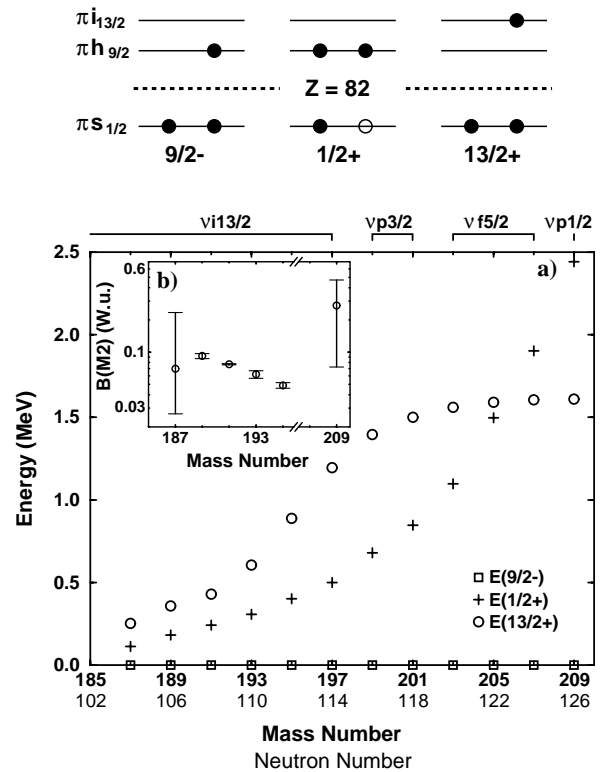


Fig. 3. a) Excitation energies of $13/2^+$ (circles) and $1/2^+$ (crosses) states in odd- A bismuth isotopes, *i.e.* relative to the $9/2^-$ ground states (squares). b) The experimental $B(M2)$ -values of the $13/2^+ \rightarrow 9/2^-$ transition are given in Weisskopf units (please note the logarithmic vertical scale and the broken horizontal axis). In the top panel the relevant proton configurations ($9/2^-$, $1/2^+$ and $13/2^+$) are shown schematically while the corresponding neutron orbitals are represented above the main figure.

$E3$ transition would be much slower than the observed values. Assuming an $E3$ transition strength of 7.2 W.u. (as measured in ^{209}Bi [21]), we indeed obtain a much longer half-life than experimentally observed, *i.e.* about 500 μs for the case of ^{187}Bi .

The systematics of low-lying $13/2^+$ states in odd-mass Bi isotopes is shown and compared to that of the $1/2^+$ states in fig. 3a. In ^{209}Bi , at the $N = 126$ shell closure, the excitation energy of both states is rather high. With decreasing neutron number the excitation energy of the $13/2^+$ state stays rather constant from ^{209}Bi to ^{199}Bi . For the lighter nuclei it drops steeply. In contrast to the $13/2^+$ state, the excitation energy of the $1/2^+$ state follows a parabolic trend, decreasing smoothly with decreasing mass. The behaviour of the $1/2^+$ intruder states towards the neutron mid-shell has been discussed in a paper by Heyde *et al.* [22] as being mainly due to the principal ingredients of the nucleon-nucleon interaction: the monopole and quadrupole interaction between protons and neutrons and the pairing between like particles.

In order to understand the behaviour of the $h_{9/2}$ and $i_{13/2}$ orbitals independently, we will discuss the systematics presented in fig. 3a more generally using the informa-

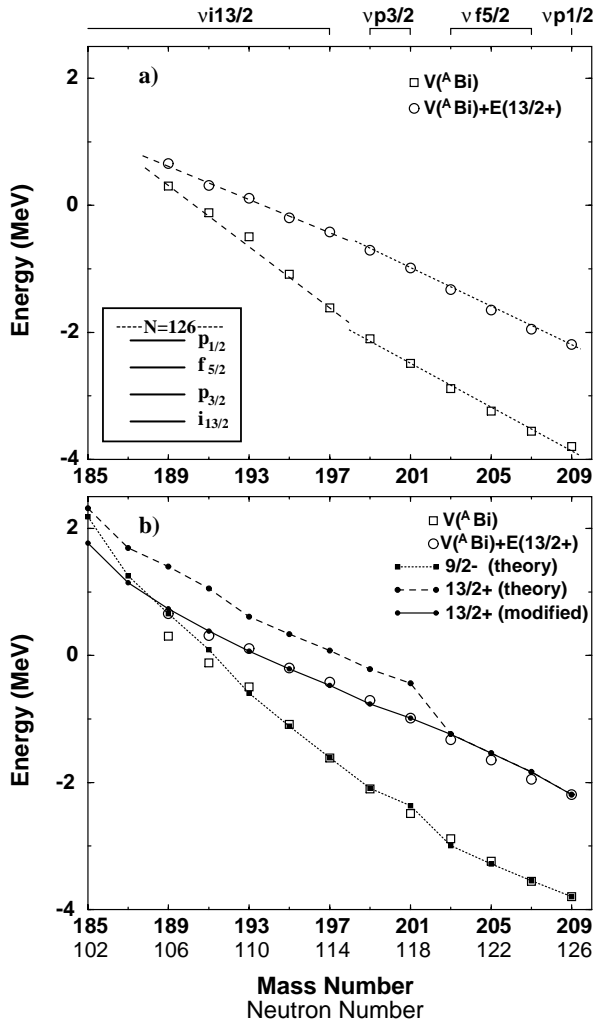


Fig. 4. a) Energies of the $9/2^-$ ground states (squares) $V(^A\text{Bi})$ in the potential of the underlying lead core, defined as $V(Z, A) = B(Z, A) - B(Z - 1, A - 1)$ with $B < 0$ being the binding energy. The energy of the $13/2^+$ states (circles) is obtained by adding the excitation energy to the term $V(^A\text{Bi})$. The lines are drawn to guide the eye only. b) Same experimental data as above, but compared to a simplified shell-model calculation (see text for further explanations).

tion available from recent nuclear mass measurements [6, 23–25]. Since these masses are not yet evaluated in a systematic way (and not part of recommended mass tables) a general uncertainty of about 200 keV could be considered as reasonable. In fig. 4, the binding energies of the $9/2^-$ and $13/2^+$ states are shown in the potential of the underlying lead core. They were obtained by adding the experimental (excitation) energy to a term $V(^A\text{Bi})$ defined as $V(Z, A) = B(Z, A) - B(Z - 1, A - 1)$ with $B < 0$ being the binding energy. The term $V(^A\text{Bi})$ corresponds to the one-proton separation energy (in the $9/2^-$ ground state), but with opposite sign. As can be seen from fig. 4a, the binding energy of the $9/2^-$ and $13/2^+$ states, both being mainly of single-proton character, decreases rapidly with decreasing mass. For $A \geq 199$ the $9/2^-$ and the $13/2^+$

states remain almost parallel, while for $A \leq 197$ the lines converge when going towards mid-shell. In ^{189}Bi the last proton is no longer bound even in the $9/2^-$ ground state. For the $13/2^+$ isomer the binding energy changes its sign in ^{193}Bi . In these cases the protons are not bound by the nuclear potential, but are quasi-bound by the Coulomb potential and the angular-momentum barrier. Due to the high angular-momentum barrier and the small Q -value for proton emission, α -decay remains the principal decay mode. Only for the $1/2^+$ state in ^{185}Bi , with a Q -value of 1.594 MeV, is proton emission observed [7].

In the following we will try to understand this systematic behaviour from the properties of the nucleon-nucleon interaction. As can be seen from the orbitals indicated on top of fig. 4, the key interactions for $A \leq 197$ are $\pi h_{9/2} \otimes \nu i_{13/2}$ and $\pi i_{13/2} \otimes \nu i_{13/2}$, respectively. In both cases the binding energy is increasing when filling the $i_{13/2}$ orbital with pairs of neutrons, but the interaction with the $h_{9/2}$ proton is stronger than with the $i_{13/2}$ proton, leading to different slopes for the binding-energy curves. This behaviour is possibly related to the spin-flip involved in the $\pi h_{9/2} \otimes \nu i_{13/2}$ case, which could lead to a stronger attraction than in the process that preserves the relative orientation of spin and orbital angular momentum. A similar interpretation has been recently used by Otsuka *et al.* to explain the disappearance of the $N = 8, 20$ shell gaps in light neutron-rich nuclei [26], but for the specific case of spin-orbit partners. For $A \geq 199$, the active neutron orbitals are $p_{3/2}$, $f_{5/2}$ and $p_{1/2}$, all which have low spin. The interaction of neutrons in these orbitals with either the $\pi h_{9/2}$ or the $\pi i_{13/2}$ is comparable, and is less attractive than for the $i_{13/2}$ neutrons. Therefore, less binding energy is gained per $p_{3/2}$, $f_{5/2}$ or $p_{1/2}$ neutron pair compared to the $i_{13/2}$ neutrons. In fig. 3a this is reflected by the approximately constant excitation energy of the $13/2^+$ state for $199 \leq A \leq 209$.

In order to confirm this interpretation, we have also performed a (simplified) shell-model calculation, since a full shell-model calculation including the high-spin proton and neutron orbitals involves very large dimensions. Calculations using a more complete basis are under preparation and will be presented in a forthcoming paper. Here, we restrict our model space to $\pi(h_{9/2}, i_{13/2})$ and $\nu(p_{1/2}, f_{5/2}, p_{3/2}, i_{13/2})$ orbitals. In addition, no excitations of the neutrons between the active orbitals were allowed. A realistic residual interaction of H7B type [27] has been used for both the proton-neutron and neutron-neutron system. The single-particle energies have been adjusted to fit the levels experimentally known in ^{209}Bi [28]. The $9/2^-$ and the $13/2^+$ states have been calculated in odd- A bismuth isotopes from $A = 185$ to $A = 209$ filling the neutron orbitals in the order indicated in the inset on fig. 4a. The results are compared to the experimental data in fig. 4b.

It is striking how well this simple calculation agrees with the experimental data for the $9/2^-$ states. Only when approaching the proton drip line a small deviation is discernible, which could be related to the onset of deformation. For the $13/2^+$ states the different slopes are also very well reproduced, but an energy shift occurs between mass

numbers 201 and 203, *i.e.* when going from the $f_{5/2}$ to the $p_{3/2}$ neutron orbital. The energy difference between the calculated and experimental points appears to be almost constant below $A = 201$. This leads us to the conclusion that the monopole strength of the $\pi i_{13/2} \otimes \nu f_{5/2}$ matrix elements is overestimated. Decreasing the corresponding interaction strength by 90 keV (*i.e.* $\sim 30\%$) leads to an almost perfect agreement with the data, as shown by the solid line in fig. 4b.

With this rather simple model a very good overall description of the valence proton states in the potential of the underlying lead core could be obtained. This shows that the behaviour of the $9/2^-$ and $13/2^+$ states is mainly determined by the proton-neutron interaction and correlations of recoupled states within a single shell. Mixing between different neutron shells, which is very important to describe the absolute binding energies, has not been included and seems not to play a major role when the energies are regarded relative to the lead core. The excellent agreement is even more surprising since the lightest Bi isotopes are known to quickly develop deformation as indicated by rotational bands built on the valence proton states in $^{189,191,193}\text{Bi}$ [11, 19, 29]. This seems to indicate that these states are still located in the spherical potential well at least at the bandhead; the loosely bound valence proton might have very little core polarisability and a sizeable deformation is only obtained by breaking the lead core. Measuring the quadrupole moments of the $13/2^+$ isomers in light-Bi isotopes would address this question.

Finally, we discuss the $B(M2)$ transition strength in the chain of odd- A Bi isotopes as presented in fig. 3b. The $13/2^+ \rightarrow 9/2^-$ $M2$ transition is observed in stable ^{209}Bi [28], but for the isotopes with $197 \leq A \leq 207$ the $|\pi h_{9/2} \otimes \nu 2^+; 11/2^- \rangle$ and $|\pi h_{9/2} \otimes \nu 2^+; 13/2^- \rangle$ configurations are lower in energy than the $13/2^+$ state [5]. Therefore, the $13/2^+$ state can decay by other (faster) transitions than the one directly to the ground state, and consequently the $M2$ decay is not observed. In ^{195}Bi the $13/2^+$ states is again lower in energy and the isomeric $M2$ transition is observed in all isotopes down to ^{187}Bi .

From the measured half-lives $B(M2)$ -values of 0.092 ± 0.005 W.u. and $0.07_{-0.04}^{+0.17}$ W.u. have been deduced for ^{189}Bi and ^{187}Bi , respectively, assuming a pure $M2$ multipolarity. This is in agreement with the values of other light-bismuth nuclei [19, 20, 29], which have generally a hindrance factor between 10 and 20. Compared to the stable isotope ^{209}Bi , where the $M2$ transition is mainly due to the transition of a single proton between the $i_{13/2}$ and $h_{9/2}$ states, the $B(M2)$ -values in light bismuth isotopes are reduced by more than a factor of 3. This (additional) hindrance might be explained by a mixing of the single-particle states with other configurations. Since only very selected orbitals are coupled by strong $M2$ transitions, mixing will lead to a reduced $M2$ strength in most cases. As an example, particle octupole-vibration coupling [30] is well known to be important in the lead region. Due to this coupling contributions to the $13/2^+$ state from $|\pi f_{7/2} \otimes 3^-; 13/2^+ \rangle$ and $|\pi h_{9/2} \otimes 3^-; 13/2^+ \rangle$ are expected, which would both decrease the $M2$ strength.

We hope to obtain a deeper insight into the $M2$ matrix elements from a more complete shell-model calculation.

4 Conclusion

Isomeric states in $^{187,189}\text{Bi}$ have been studied by delayed γ -ray spectroscopy combined with the RDT technique. Long-lived isomers decaying via γ -rays to the ground state have been observed. They are interpreted as $13/2^+$ states being mainly due to a valence proton excitation into the $i_{13/2}$ orbital. The strength of the corresponding $M2$ decay has also been deduced. The $9/2^-$ and $13/2^+$ states have been described in the potential of the underlying lead core. Simplified shell-model calculations reproduce very well the systematics.

The authors are grateful to the staff of the Jyväskylä accelerator laboratory for providing excellent running conditions. This work has been supported by the European Fifth Framework Programme “Improving Human Potential - Access to Research Infrastructure”; Contract No. HPRI-CT-1999-00044 and by the Academy of Finland under the Finnish Centre of Excellence Programme 2000-2005 (Project No. 44875, Nuclear and Condensed Matter Physics Programme at JYFL). The authors would also like to thank H. Grawe, E. Caurier and F. Nowacki for enlightening discussions.

References

1. A.N. Andreyev *et al.*, Nature (London) **405**, 430 (2000).
2. R.G. Allatt *et al.*, Phys. Lett. B **437**, 29 (1998).
3. Y. Le Coz *et al.*, Eur. Phys. J. direct A **3**, 1 (1999).
4. J.L. Wood, K. Heyde, W. Nazarewicz, M. Huyse, P. Van Duppen, Phys. Rep. **215**, 101 (1992).
5. R.B. Firestone, V.S. Shirley (Editors), *Table of Isotopes*, 8th edition (Wiley, New York, 1996).
6. Yu.N. Novikov *et al.*, Nucl. Phys. A **697**, 92 (2002).
7. C.N. Davids *et al.*, Phys. Rev. Lett. **76**, 592 (1996).
8. G.L. Poli *et al.*, Phys. Rev. C **63**, 044304 (2001).
9. E.S. Paul *et al.*, Phys. Rev. C **51**, 78 (1995).
10. M. Leino *et al.*, Nucl. Instrum. Methods B **99**, 653 (1995).
11. A. Hürstel *et al.*, in preparation.
12. J. Wauters *et al.*, Phys. Rev. C **55**, 1192 (1997).
13. E. Coenen, K. Deneffe, M. Huyse, P. Van Duppen, J.L. Wood, Phys. Rev. Lett. **54**, 1783 (1985).
14. A.N. Andreyev *et al.*, J. Phys. G **25**, 835 (1999).
15. A.N. Andreyev *et al.*, Eur. Phys. J. A **10**, 129 (2001).
16. J.C. Batchelder *et al.*, Eur. Phys. J. A **5**, 49 (1999).
17. K.H. Schmidt, C.C. Sahn, K. Pielenz, H.G. Clerc Z. Phys. A **316**, 19 (1984).
18. K. Heyde, P. Van Isacker, M. Waroquier, J.L. Wood, R.A. Meyer, Phys. Rep. **102**, 291 (1983).
19. P. Nieminen *et al.*, Acta Phys. Pol. B **32**, 1019 (2001).
20. T. Lönnroth *et al.*, Phys. Rev. C **33**, 1641 (1986).
21. J.W. Hertel, D.G. Fleming, J.P. Schiffer, H.E. Gove, Phys. Rev. Lett. **23**, 488 (1969).
22. K. Heyde, J. Ryckebusch, M. Waroquier, J.L. Wood, Nucl. Phys. A **484**, 275 (1988).

23. G. Audi, A.H. Wapstra, Nucl. Phys. A **595**, 409 (1995).
24. T. Radon *et al.*, Nucl. Phys. A **677**, 75 (2000).
25. S. Schwarz *et al.*, Nucl. Phys. A **693**, 533 (2001).
26. T. Otsuka, R. Fujimoto, Y. Utsuno, A. Brown, M. Honna, T. Mizusaki, Phys. Rev. Lett. **87**, 082502-1 (2001).
27. A. Hosaka, K.I. Kubo, H. Toki, Nucl. Phys. A **444**, 76 (1985).
28. M.J. Martin, Nucl. Data Sheets **63**, 723 (1991).
29. P. Nieminen *et al.*, to be published in *Proceedings of the Conference on Frontiers of Nuclear Structure, Berkeley (2002)*.
30. A. Bohr, B.R. Mottelson, *Nuclear Structure*, Vol. **2** (W.A. Benjamin, Inc., 1975) p. 416.